

Microwave and infrared dielectric response of monoclinic bismuth zinc niobate based pyrochlore ceramics with ion substitution in A site

Hong Wang^{a)}

Electronic Materials Research Laboratory, Key Laboratory of the Ministry of the Education, Xi'an Jiaotong University, Xi'an 710049, China

Stanislav Kamba^{b)}

Institute of Physics ASCR, Na Slovance 2, 18221 Prague 8, Czech Republic

Meiling Zhang and Xi Yao

Electronic Materials Research Laboratory, Key Laboratory of the Ministry of the Education, Xi'an Jiaotong University, Xi'an 710049, China

Sergey Denisov, Filip Kadlec, and Jan Petzelt

Institute of Physics ASCR, Na Slovance 2, 18221 Prague 8, Czech Republic

(Received 6 December 2005; accepted 24 May 2006; published online 9 August 2006)

It is well known that the cubic pyrochlore $\text{Bi}_{1.5}\text{ZnNb}_{1.5}\text{O}_7$ exhibits higher permittivity and dielectric loss than monoclinic $\text{Bi}_2\text{Zn}_{2/3}\text{Nb}_{4/3}\text{O}_7$ due to structural disorder in the A sites of $\text{Bi}_{1.5}\text{ZnNb}_{1.5}\text{O}_7$. We have studied systematically the impact of the ion substitution in the A site of monoclinic $\text{Bi}_2\text{Zn}_{2/3}\text{Nb}_{4/3}\text{O}_7$ on the structure and microwave dielectric properties. It is shown that the structure and permittivity of $(\text{Bi}_{1.92}\text{M}_{0.08})(\text{Zn}_{0.64}\text{Nb}_{1.36})\text{O}_7$ ($M=\text{Zn, Ca, Cd, Sr, Ba}$) ceramics remain almost the same as in $\text{Bi}_2\text{Zn}_{2/3}\text{Nb}_{4/3}\text{O}_7$; only the Ba substituted ceramics have higher permittivity due to multiphase structure. Microwave dielectric properties were compared with complex dielectric response in terahertz and infrared frequency range of 0.1–100 THz, which allows us to estimate intrinsic and extrinsic contributions to microwave dielectric losses. The best microwave properties were obtained in $(\text{Bi}_{1.92}\text{Ca}_{0.08})(\text{Zn}_{0.64}\text{Nb}_{1.36})\text{O}_7$ with $\epsilon=76$, $Qf \geq 5000$ (sintered below 950 °C), which is promising for microwave low temperature cofiring ceramic application. © 2006 American Institute of Physics. [DOI: 10.1063/1.2219161]

I. INTRODUCTION

With the recent development of low temperature cofiring ceramic (LTCC) devices, the demands for materials that can be cofired with metal electrodes and other ceramics are increasing in the past decade. Bismuth based pyrochlore ceramics thus attracted attention due to their excellent dielectric properties and lower firing temperatures as promising candidates for LTCC and microwave (MW) passive components. $\text{Bi}_2\text{O}_3\text{--ZnO--Nb}_2\text{O}_5$ (BZN) based pyrochlore ceramics were explored in 1970's by Chinese engineers for low firing temperature multilayer capacitors.¹ Previous work revealed that there are two main phases in the system: a cubic pyrochlore phase $\text{Bi}_{1.5}\text{ZnNb}_{1.5}\text{O}_7$ (dielectric constant ~ 150 , temperature coefficient of permittivity (α_ϵ) ~ -400 ppm/°C) and a monoclinic zirconolite-like pyrochlore phase $\text{Bi}_2\text{Zn}_{2/3}\text{Nb}_{4/3}\text{O}_7$ [dielectric constant ~ 80 , $\alpha_\epsilon \sim +150$ ppm/°C (Refs. 2 and 3)]. The cubic structure of BZN ($Fd\bar{3}m\text{--}O_h^7$), $Z=8$, and monoclinic zirconolite-like structure ($C2/c\text{--}C_{2h}^6$) were studied in detail.^{4–7} In cubic pyrochlore BZN the Bi and Zn atoms in the A positions are disordered among six closely spaced equivalent sites and the O' atoms from the $A_2\text{O}'$ tetrahedral network among 12 sites,⁴ while

the Zn atoms prefer the B site to the A site.⁸ Broadband dielectric measurements of cubic BZN revealed a wide dielectric relaxation which slows down and broadens on cooling.⁹ The relaxation has its origin in hopping of atoms in the A and O' sites of pyrochlore structure among several potential minima. The broad distribution of relaxation frequencies is a consequence of distribution of the barrier heights for hopping of disordered atoms due to random fields from inhomogeneous distribution of Zn^{2+} atoms and vacancies at Bi^{3+} sites.^{9–11} Disorder of these atoms is only slightly influenced by Ti substitution in the B sites, while the activation energy for hopping of disordered atoms decreases and MW permittivity increases with Ti substitution due to enhanced polar phonon and dielectric relaxation contributions.¹¹ The dielectric permittivity was observed to be tunable by the electric field, while dielectric losses remain almost field independent.^{12,13}

No dielectric relaxation was observed in monoclinic BZN,¹⁴ which corresponds also to a better ordered crystal structure.⁷ Therefore the dielectric losses and $|\alpha_\epsilon|$ are much lower in monoclinic than in cubic BZN. Low sintering temperature is promising for LTCC application of monoclinic BZN in MW devices. In this work, we will present the results of the effect of ion substitutions in the A site of BZN monoclinic pyrochlores on MW, terahertz and infrared (IR) dielectric properties, and we will show that the best MW quality can be achieved in $(\text{Bi}_{1.92}\text{Ca}_{0.08})(\text{Zn}_{0.64}\text{Nb}_{1.36})\text{O}_7$.

^{a)}Electronic mail: hwang@mail.xjtu.edu.cn

^{b)}Electronic mail: kamba@fzu.cz

TABLE I. Dielectric properties of typical compositions in the BZN system.

| Compositions | Phase | ϵ_r | $\tan\delta$ | α_e (ppm/°C) | GHz | | |
|--|--------------------|--------------|---------------------|---------------------|--------------|------|------|
| | | | | | ϵ_r | Q | Qf |
| (Bi _{1.5} Zn _{0.5})(Zn _{0.5} Nb _{1.5})O ₇ | α | 145 | $<1 \times 10^{-3}$ | -520 | 140 | 35 | 160 |
| (Bi _{1.8} Zn _{0.2})(Zn _{0.6} Nb _{1.4})O ₇ | α - β | 100 | $<6 \times 10^{-4}$ | -37 | 97 | 80 | 300 |
| Bi ₂ (Zn _{2/3} Nb _{4/3})O ₇ | β | 80 | $<6 \times 10^{-4}$ | +230 | 76 | 1000 | 3700 |

II. EXPERIMENT

The ceramics of BZN-based composition (Bi_{1.92}M_{0.08}) × (Zn_{0.64}Nb_{1.36})O₇ ($M = \text{Zn, Ca, Cd, Sr, Ba}$) with different M ions in the A site were synthesized by conventional ceramic technology. High purity Bi₂O₃, ZnO, CaO, CdO, SrCO₃, BaCO₃, and reagent grade Nb₂O₅ were used as starting materials. The constituent oxides were weighed out in proper ratio and mixed with alcohol using agate milling media. The slurries were filtered and dried under an IR lamp. The dried powders were calcined in air from 750 to 850 °C for 2 h. Then the powders were pressed into disks of 10 mm in diameter. The disks were finally sintered from 900 to 1000 °C for 2 h.

The phase structures of BZN samples were characterized by X-ray diffractometry. The X-ray diffraction patterns were obtained using a Rigaku D/MAX-2400 X-ray diffractometer with Cu $K\alpha$ radiation with $2\theta = 0.02^\circ$ step width.

The dielectric properties at low frequencies were measured using a high-precision 4284A LCR meter in the range of 1 KHz–1 MHz. The electrical resistivity was obtained by an HP 4339A high-resistance meter under a measuring voltage of 100 V dc for 1 min. Dielectric measurements in the high-frequency (HF) range (1 MHz–1.8 GHz) and at terahertz frequencies are using the same methods, as described in detail in our another work.¹¹ Our terahertz technique allows us to determine the complex dielectric response, $\epsilon^*(\omega) = \epsilon'(\omega) - i\epsilon''(\omega)$, in the range of 3–80 cm⁻¹ (0.1–2.4 THz).

Near-normal incidence IR reflectivity spectra at room temperature were obtained using the same method as that in Ref. 11. Reflectivity spectra were fitted together with the $\epsilon^*(\omega)$ spectra in the terahertz range using a sum of quasi-harmonic damped oscillators

$$\epsilon^*(\omega) = \sum_{j=1}^n \frac{\Delta\epsilon_j \omega_j^2}{\omega_j^2 - \omega^2 + i\omega\gamma_j} + \epsilon_\infty, \quad (1)$$

where $\epsilon^*(\omega)$ is related to reflectivity $R(\omega)$ by

$$R(\omega) = \left| \frac{\sqrt{\epsilon^*(\omega)} - 1}{\sqrt{\epsilon^*(\omega)} + 1} \right|^2. \quad (2)$$

ω_j , γ_j , and $\Delta\epsilon_j$ are the frequencies, damping, and dielectric strength of the j th polar phonon, respectively. The high-frequency permittivity ϵ_∞ results from electronic absorption processes at frequencies much higher than phonon frequencies (typically in UV-Vis range).

III. RESULTS AND DISCUSSION

The dielectric properties in megahertz and MW ranges of pure BZN ceramics crystallizing in cubic, monoclinic and in both phases are listed in Table I. It is seen that the cubic pyrochlore has much lower MW Q value than monoclinic pyrochlore, although they both have similar low dielectric loss in the megahertz range. This is due to MW relaxation in cubic BZN described already in Refs. 9 and 14. Note that the ceramics with mixed cubic α and monoclinic β phases display an intermediate permittivity of 100, a low Q , but quite low and promising $\alpha_e = -37$ ppm/°C.

It is known from previous studies that the larger ions at the A sites are beneficial for the stability of the monoclinic BZN structure.^{6,15} Thus in this work we used different ions with large radii for substitution of the Zn at A sites to study the effect on MW properties while keeping the structure pure monoclinic.

The XRD patterns of the (Bi_{1.92}M_{0.08})(Zn_{0.64}Nb_{1.36})O₇ ($M = \text{Zn, Ca, Cd, Sr, Ba}$) samples are shown in Fig. 1. The crystal structure of all the samples except Ba substituted is characterized as pure monoclinic zirconolitelike pyrochlore [Powder Diffraction File 54-972 (Ref. 4)]. In the Ba²⁺ substituted sample, a second phase was observed with composition BaBi₂Nb₂O₉ (PDF 40-0355). This is due to the huge radius and polarizability of Ba²⁺ compared with Bi³⁺ and Zn²⁺. The X-ray diffraction (XRD) peaks of the Zn²⁺, Cd²⁺, Ca²⁺, and Sr²⁺ substituted compositions regularly shift to lower diffraction angles indicating that the lattice parameters of these doped samples are gradually increased, which corresponds to the gradually increasing ion radii of Zn, Cd, Ca, and Sr. In the Ba²⁺ substituted sample, no obvious shifts of the XRD peaks were observed, which can be assumed by the emergence of the second phase.

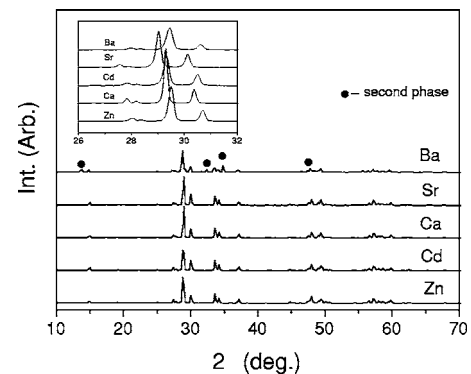


FIG. 1. XRD patterns of (Bi_{1.92}M_{0.08})(Zn_{0.64}Nb_{1.36})O₇ ($M = \text{Zn, Ca, Cd, Sr, Ba}$) ceramics.

TABLE II. Dielectric data of $(\text{Bi}_{1.92}\text{M}_{0.08})(\text{Zn}_{0.64}\text{Nb}_{1.36})\text{O}_7$ ($M=\text{Zn, Ca, Cd, Sr, Ba}$) in megahertz, MW, and terahertz ranges.

| $M=$ | Sintering Temperature (°C) | Radius of M ions (Å) | Polarizabilities of M ions | ρ (Ω cm) | Density (g/cm^3) | ε' (MHz) | ε' (GHz) | ε' (THz) | $\tan \delta$ (MHz) | Qf (GHz) | Qf (THz) | α_e (ppm/°C) |
|------|----------------------------|------------------------|------------------------------|-----------------------|------------------------------------|----------------------|----------------------|----------------------|---------------------|------------|------------|---------------------|
| Zn | 1000 | 0.75 | 2.09 | $\geq 10^{12}$ | 7.516 | 82 | 75 | 77 | 0.0014 | 1755 | 3090 | 248 |
| Cd | 980 | 1.07 | 3.40 | $\geq 10^{12}$ | 7.590 | 88 | 76 | 76 | 0.0044 | 660 | 3130 | 336 |
| Ca | 960 | 1.12 | 3.05 | $\geq 10^{12}$ | 7.440 | 80 | 76 | 76 | 0.0005 | 3989 | 3050 | 214 |
| Sr | 940 | 1.25 | 4.25 | $\geq 10^{12}$ | 7.536 | 93 | 76 | 76 | 0.0013 | 1100 | 3310 | 272 |
| Ba | 1000 | 1.42 | 6.40 | $\geq 10^{12}$ | 7.631 | 99 | 90 | 83 | 0.013 | 20 | 3660 | 819 |

It is seen in Table II that the permittivity increases with the polarizability of the M ions. megahertz permittivity is systematically higher than the gigahertz permittivity due to conductivity and other extrinsic contributions to permittivity at low frequencies; however, MW and terahertz permittivities agree with each other. This gives evidence that the MW permittivity is completely determined by the polar phonon contributions. HF dielectric data between 1 and 300 MHz (Fig. 2) show no frequency dependence of the permittivity, except for the Ba^{2+} substituted sample. This exception is due to the relaxation caused by the second $\text{BaBi}_2\text{Nb}_2\text{O}_9$ phase, which is known as relaxor ferroelectrics.¹⁶ In this case the dispersion was observed within gigahertz and terahertz ranges (see Table II) as well as in the HF range [see Fig. 2(b)].

IR reflectivity spectra (Fig. 3) show no dramatic change of the phonon structure with the substitution, which is consistent with the same monoclinic crystal structure in all samples. Only in the case of Ba substituted sample is a higher damping of all modes seen due to multiphase composition and higher disorder of the structure.

Factor group analysis of the lattice vibrations gives the following vibration modes in the Γ point of the Brillouin zone:

$$\Gamma = 34A_g(x^2, y^2, z^2, xy) + 34A_u(z) + 35B_g(xz, yz) + 35B_u(x, y).$$

It means that after subtraction of 1 A_u and 2 B_u acoustic modes we can expect 66 IR active modes in our IR spectra (and 69 modes in Raman spectra). Note that the total number of vibration modes is higher than what is expected from the number of atoms in the primitive unit cell, which is caused by the 50% occupancy of Zn atoms at the $8f$ sites.⁷ We have observed only 16 polar modes active in our IR spectra, and the list of their parameters is shown in Table III. We did not resolve all allowed modes in the spectra due to their possible overlapping and the low intensity of some of them. Nevertheless, we observed much higher number of modes than Chen *et al.*,¹⁷ who found only three highly damped modes above 300 cm^{-1} in the IR reflectivity of the ceramics and in the IR transmission of thin films. Also, their sample exhibited a lower permittivity (only 65 in the MW range), which indicates a multiphase composition of their samples. It is also the reason for the higher damping of their polar modes.

Figure 4 shows calculated permittivity $\varepsilon'(\omega)$ and loss $\varepsilon''(\omega)$ spectra obtained from our fits to experimental results based on the IR reflectivity, terahertz transmittance, and MW

measurements. MW and terahertz permittivities are equal in all the samples except for the Ba substituted one, which gives evidence that only this sample exhibits a dielectric relaxation below the terahertz region (probably due to the presence of the second phase with relaxor ferroelectric properties). The ε'' values extrapolated from the IR and terahertz spectra down to MW range allow us to estimate intrinsic dielectric loss in the MW range. In Fig. 4(b) one can see a

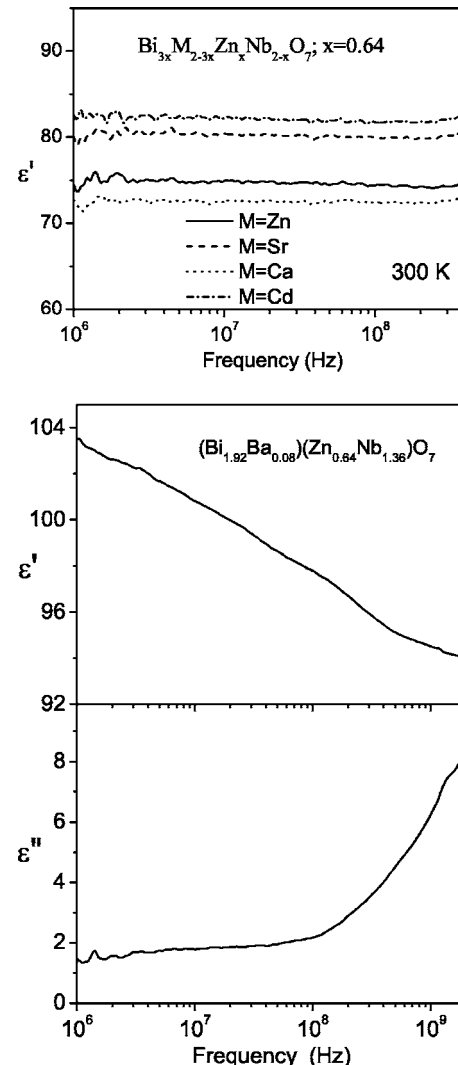


FIG. 2. HF dielectric spectra of (a) $(\text{Bi}_{1.92}\text{M}_{0.08})(\text{Zn}_{0.64}\text{Nb}_{1.36})\text{O}_7$ ($M=\text{Zn, Ca, Cd, Sr}$) and (b) $(\text{Bi}_{1.92}\text{Ba}_{0.08})(\text{Zn}_{0.64}\text{Nb}_{1.36})\text{O}_7$ ceramics. Dielectric loss spectra of ceramics with $M=\text{Zn, Sr, Ca, and Cd}$ were below the detection limit of our setup.

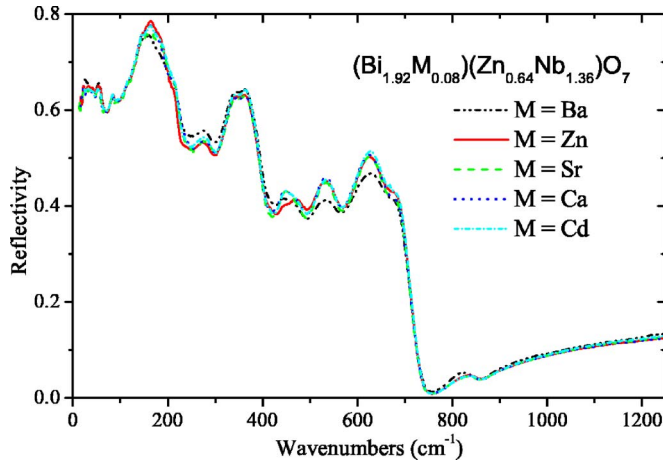


FIG. 3. (Color online) Room temperature IR reflectivity spectra of $(\text{Bi}_{1.92}\text{M}_{0.08})(\text{Zn}_{0.64}\text{Nb}_{1.36})\text{O}_7$ ($M=\text{Zn}, \text{Ca}, \text{Cd}, \text{Sr}, \text{Ba}$) ceramics.

disagreement between the extrapolated and experimental MW losses in all ceramics due to the high extrinsic dielectric losses. The best correspondence was observed in the Ca^{2+} substituted sample. It explains why the best Qf (5580 GHz) among of all the studied ceramics was observed in this sample: the extrinsic contribution to the MW loss is apparently the smallest in the Ca-substituted sample.

IV. CONCLUSION

The MW dielectric behavior of $(\text{Bi}_{1.92}\text{M}_{0.08}) \times (\text{Zn}_{0.64}\text{Nb}_{1.36})\text{O}_7$ ($M=\text{Zn}, \text{Ca}, \text{Cd}, \text{Sr}, \text{Ba}$) ceramics was systematically investigated. MW dielectric properties were compared with the complex dielectric response in the 0.1–100 THz range. The dielectric spectra obtained in a broad spectral range show that the best MW properties, i.e., the lowest dielectric losses, were observed in the Ca-substituted monoclinic BZN ($\epsilon \sim 75$, $Qf \geq 5000$ GHz), apparently due to the reduced extrinsic contributions to dielectric losses.

TABLE III. Mode parameters of polar phonons in $(\text{Bi}_{1.92}\text{Zn}_{0.08}) \times (\text{Zn}_{0.64}\text{Nb}_{1.36})\text{O}_7$. $\epsilon_\infty = 5.64$.

| No. of modes | ω_j (cm^{-1}) | $\Delta\epsilon_j$ | γ_j (cm^{-1}) |
|--------------|---------------------------------|--------------------|---------------------------------|
| 1 | 51.0 | 19.9 | 45.9 |
| 2 | 58.1 | 4.6 | 12.7 |
| 3 | 67.6 | 0.8 | 26.7 |
| 4 | 85.8 | 0.9 | 8.3 |
| 5 | 92.7 | 2.7 | 21.5 |
| 6 | 146.3 | 33.4 | 46.0 |
| 7 | 203.5 | 0.5 | 24.0 |
| 8 | 239.4 | 1.1 | 46.1 |
| 9 | 270.6 | 1.7 | 50.2 |
| 10 | 328.7 | 4.0 | 68.1 |
| 11 | 429.0 | 0.3 | 60.0 |
| 12 | 441.7 | 0.04 | 23.2 |
| 13 | 462.6 | 0.34 | 49.4 |
| 14 | 518.1 | 1.01 | 84.7 |
| 15 | 596.7 | 0.50 | 71.0 |
| 16 | 666.1 | 0.03 | 40.6 |

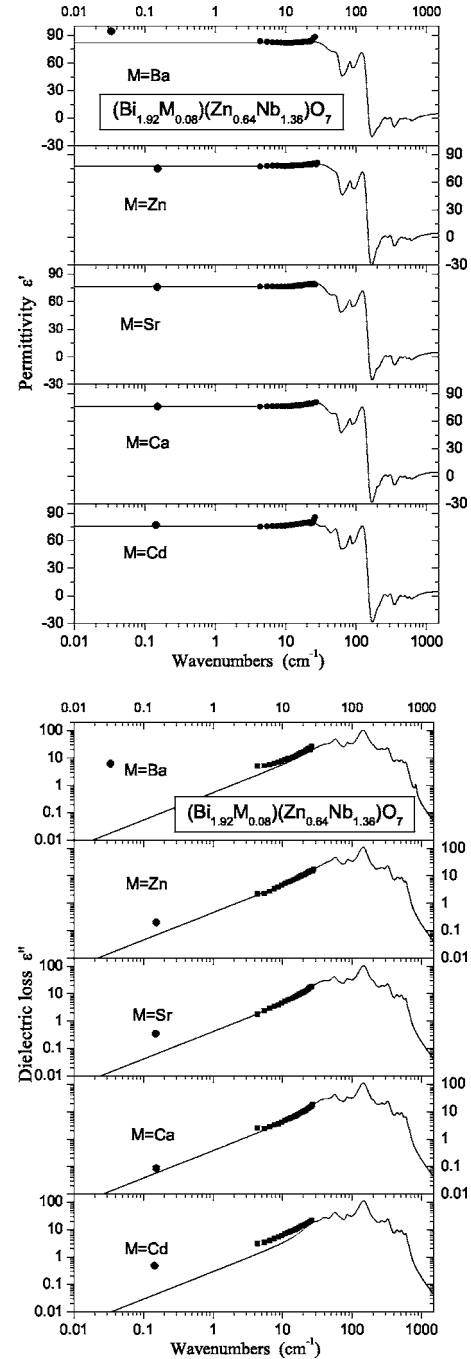


FIG. 4. (a) Real and (b) imaginary parts of the complex dielectric spectra of $(\text{Bi}_{1.92}\text{M}_{0.08})(\text{Zn}_{0.64}\text{Nb}_{1.36})\text{O}_7$ ($M=\text{Zn}, \text{Ca}, \text{Cd}, \text{Sr}, \text{Ba}$) ceramics. Full symbols are experimental MW and terahertz data; solid lines are the results of the fits to IR and terahertz spectra.

ACKNOWLEDGMENTS

This work was supported by the National 973 project of China under Grant No. 2002CB613302, NSFC project of China under Grant No. 50572085, and Grant Agency of the Czech Republic (Project Nos. 202/04/0993 and AVOZ 10100520).

¹Z. P. Wang and S. Y. Zhang, Electronic Components and Materials (in Chinese) **1**, 11 (1979).

²X. Wang, H. Wang, and X. Yao, J. Am. Ceram. Soc. **80**, 2745 (1997).

³D. Liu, Y. Liu, S. Huang, and X. Yao, J. Am. Ceram. Soc. **76**, 2129 (1993).

- ⁴I. Levin, T. G. Amos, J. C. Nino, T. A. Vanderah, C. A. Randall, and M. T. Lanagan, *J. Solid State Chem.* **168**, 69 (2002).
- ⁵R. L. Withers, T. R. Welberry, A.-K. Larsson, Y. Liu, L. Norén, H. Rundlöf, and F. J. Frank, *J. Solid State Chem.* **177**, 231 (2004).
- ⁶H. Wang, X. Wang, and X. Yao, *Ferroelectrics* **195**, 19 (1997).
- ⁷I. Levin, T. G. Amos, J. C. Nino, T. A. Vanderah, I. M. Reaney, C. A. Randall, and M. T. Lanagan, *J. Mater. Res.* **17**, 1406 (2002).
- ⁸H. Wang, H. Du, and X. Yao, *Mater. Sci. Eng., B* **B99**, 20 (2003).
- ⁹S. Kamba *et al.*, *Phys. Rev. B* **66**, 054106 (2002).
- ¹⁰J. C. Nino, M. T. Lanagan, C. A. Randall, and S. Kamba, *Appl. Phys. Lett.* **81**, 4404 (2002).
- ¹¹H. Wang *et al.*, *J. Appl. Phys.* **99**, 1 (2006).
- ¹²W. Ren, S. Trolier-McKinstry, C. A. Randall, and T. R. ShROUT, *J. Appl. Phys.* **89**, 767 (2001).
- ¹³A. K. Tagantsev, J. Lu, and S. Stemmer, *Appl. Phys. Lett.* **86**, 032901 (2005).
- ¹⁴J. C. Nino, M. T. Lanagan, and C. A. Randall, *J. Appl. Phys.* **89**, 4512 (2001).
- ¹⁵H. Wang, Ph.D. thesis, The Xi'an Jiaotong University, 1998.
- ¹⁶A. L. Kholkin, M. Avdeev, M. E. V. Costa, J. L. Baptista, and S. N. Dorogovtsev, *Appl. Phys. Lett.* **79**, 662 (2001).
- ¹⁷Y.-Ch. Chen, H.-L. Liu, H.-F. Cheng, and I.-N. Lin, *J. Eur. Ceram. Soc.* **21**, 1711 (2001).